Stable ^{85}Rb micro vapour cells: fabrication based on anodic bonding and application in chip-scale atomic clocks*

Su Juan(苏 娟)[a], Deng Ke(邓 科)[b], Guo Deng-Zhu(郭等柱)[a]†,
Wang Zhong(汪 中)[b], Chen Jing(陈 兢)[c], Zhang Geng-Min(张耿民)[a], and Chen Xu-Zong(陈徐宗)[b]

[a] *Key Laboratory for the Physics & Chemistry of Nanodevices, School of Electronics Engineering & Computer Science, Peking University, Beijing* 100871, *China*

[b] *Institute of Quantum Electronics, School of Electronics Engineering & Computer Science, Peking University, Beijing* 100871, *China*

[c] *Department of Microelectronics, School of Electronics Engineering & Computer Science, Peking University, Beijing* 100871, *China*

(Received 10 May 2010; revised manuscript received 21 June 2010)

We describe the microfabrication of ^{85}Rb vapour cells using a glass-silicon anodic bonding technique and *in situ* chemical reaction between rubidium chloride and barium azide to produce Rb. Under controlled conditions, the pure metallic Rb drops and buffer gases were obtained in the cells with a few mm^3 internal volumes during the cell sealing process. At an ambient temperature of 90 °C the optical absorption resonance of ^{85}Rb D1 transition with proper broadening and the corresponding coherent population trapping (CPT) resonance, with a signal contrast of 1.5% and linewidth of about 1.7 kHz, have been detected. The sealing quality and the stability of the cells have also been demonstrated experimentally by using the helium leaking detection and the after-9-month optoelectronics measurement which shows a similar CPT signal as its original status. In addition, the physics package of chip-scale atomic clock (CSAC) based on the cell was realized. The measured frequency stability of the physics package can reach to 2.1×10^{-10} at one second when the cell was heated to 100 °C which proved that the cell has the quality to be used in portable and battery-operated devices.

Keywords: ^{85}Rb Micro vapour cell, anodic bonding, coherent population trapping chip-scale atomic clock, frequency stability

PACC: 0710C, 0630F, 3290, 0730

1. Introduction

In recent years, chip-scale atomic clocks (CSACs) have been increasingly recognized to be significant in the future man-portable electronic devices such as the synchronization of telecommunications networks and global positioning system (GPS) receivers in both military[1] and civilian[2] applications with advantages of small size, ultra-low power consumption, and low fabricating cost. Miniaturization of the traditional microwave-excited atomic clocks has been limited by the atomic vapour cell requirements, in which the cavity dimension must be as long as the wavelength of the excitation source ($\sim$ 1 cm). As indicated by Kitching and his coworkers,[3] the vapour cells could be further miniaturized without such a limitation by introducing the coherent population trapping (CPT) technique in operating the atomic clocks. Thus, the development of CPT-based atomic clocks has caused great interests during the past few years.[4−7]

In the CPT atomic clock, two coaxial laser beams, which are usually emitted from a local-oscillator-modulated semiconductor laser, pass through the atomic vapour cell to generate a coherent 'dark state' in the atomic hyperfine transition at their different frequencies. When the frequency difference of the two beams is equal to the frequency separation of the hyperfine splitting of the atomic ground state, the atoms are optically pumped into CPT state, a reduction of the optical absorption could be observed, as shown in Fig. 1. Such a working principle of CPT atomic clocks allows the vapour cells to be decreased down to submilimeter scale. However, shrinking the vapour cell size down to millimeter and sub-

*Project supported by National 863/973 Plans Projects (Grant Nos. 2006AA04Z361, 2006CB932402) and NSFC (Grant No. 60971002).

†Corresponding author. E-mail: guodz@pku.edu.cn

© 2010 Chinese Physical Society and IOP Publishing Ltd

milimeter scales is technically difficult by using conventional glass-blowing techniques. Thus, a novel microfabrication process of the atomic vapour cell by using the techniques of micro-electromechanical systems (MEMS) has been proposed to create a 'glass–silicon-glass' sandwich structures with alkali atoms (cesium (Cs), or rubidium (Rb)) and buffer gases stored in the cavity of silicon plate. Considering the chemically-active properties of Cs and Rb, and the conflict between high temperature requirements during the anodic bonding process and their low melting points, to fill alkali atoms into the cavities has been proven to be a technique challenge.

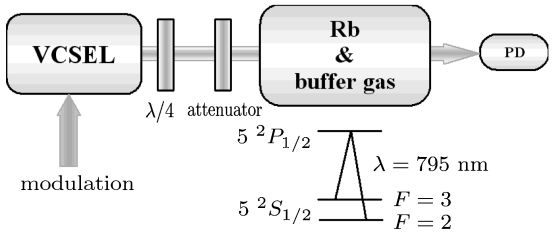


Fig. 1. Schematic illustration of the working principle of a CPT-based atomic clock.

Several cell-filling techniques have been explored for the microfabrication of MEMS vapour cells. Unlike the direct Cs filling method at the very beginning,[8,9] Liew *et al.* for the first time realized the sandwich-structured Cs vapour cells by *in situ* chemical reaction between cesium chloride (CsCl) and barium azide (BaN_6) during the sealing process,[10] and more recently, they produced Cs and buffer gas nitrogen by photolysis of cesium azide after the sealing process.[11] The similar photo-induced reaction method for Cs releasing after the cell sealing has been also used by Douahi and his coworkers.[12] As an option, Gong *et al.* proposed an electrolytic method to produce Cs after the cells sealing.[13]

We noticed that most of the relative literatures are directly involved in the microfabrication and application of Cs vapour cells due to Cs' s vapour pressure is higher than Rb' s at the same temperature, which can lower the operating temperature of the cells in the CSACs. However, as indicated by Lutwak *et al.*, due to Cs' s higher Zeeman degeneracy compared with Rb' s, the CPT resonance contrast for both D1 and D2 excitation in Cs are lower than that in Rb.[14] Moreover, it has been proven theoretically and experimentally that the CPT signal strength excited on the D1 transition is much higher than that on D2 transition in Rb.[15] Therefore, microfabrication of Rb cells is also of significance in developing CSACs based on CPT techniques, and has attracted intense research interest recently. Lee *et al.* transferred liquid Rb into the cells by using microfluidic channels after the cell formation.[16] Radhakrishnan and Lal enclosed Rb into wax in glovebox followed by laser ablation to release Rb into the cell, but they only obtained the ^{87}Rb D2 absorption spectrum without CPT signals.[17] More recently, Knappe *et al.* filled the cells with the mixture powder of 87-rubidium chloride (^{87}RbCl) and BaN_6 to produce pure ^{87}Rb through their chemical reaction during the cell sealing process, and realized the first ^{87}Rb-based CSAC physics package, which operated at 120 °C.[18] Our group has also been engaging in developing the CPT-based Rb CSACs and its related research for several years.[19−22] We choose ^{85}Rb rather than traditional ^{87}Rb because ^{85}Rb needs not to be purified to realize CPT-based atomic clock compared with ^{87}Rb under the same experimental conditions,[23] which can lower the cost of the atomic clock. In addition, the hyperfine splitting frequency of ^{85}Rb's ground state is much lower than ^{87}Rb, which can lower the power requirement of the laser modulation sources and it is more effective for the circuit designs of radio frequency (RF).[6]

In this paper, we present the fabrication of our ^{85}Rb vapour cells based on MEMS technology. By using the similar method employed by Knappe *et al.*[18] and controlling the pre-treatment and reaction conditions, we achieved appropriate buffer gas pressure of nitrogen (N_2) in the sealed 1 mm long cells so that the CPT signal of ^{85}Rb D1 line has been obtained at 90 °C with linewidth of about 1.7 kHz. The sealing quality of the cell is tested by helium leaking detection, and the actual lifetime of the cells is verified to be more than 9 months through CPT signal detection. We also realized the ^{85}Rb-based CSAC physics package using this vapour cell and measured its frequency stability. When the cell was heated to 100 °C, the Allan deviation can reach to 2.1×10^{-10} at 1 s, and the deviation is in the scale of 1×10^{-11} to 1×10^{-10} at longer times ($\tau > 50$ s).

2. Experimental procedure

2.1. Principle of anodic bonding

Anodic bonding, which is also called field-assisted bonding, was first proposed in 1969 by Wallis and Pomerantz.[24] It is a welding technology to bond metals or nonmetals under lower temperature (200 °C–

500 °C) and a high voltage (300 V–1500 V). It has been widely used in fabrication and packaging of MEMS devices for its high bonding quality. Silicon (Si) and glass are typical materials used in anodic bonding. The principle of the bonding process is shown in Fig. 2. With the increase of temperature, Na^+ ions in the glass become mobile so that they are attracted toward the cathode connected to the glass, which leave O^{2-} anions at the glass side of the Si–glass interface to form a space charge region. This creates an equivalent positive charge on the Si side, which results in a high electric field across the interface section. The electrostatic force caused by this electric field drives the two sides of the Si–glass interface closer enough so that the oxidation of Si by O^{2-} anions is expected to occur, which contributes to the formation of a thin oxide layer to bond the two materials together firmly.[25,26] Based on this principle, we designed our own high vacuum anodic bonding setup to seal the MEMS cells.

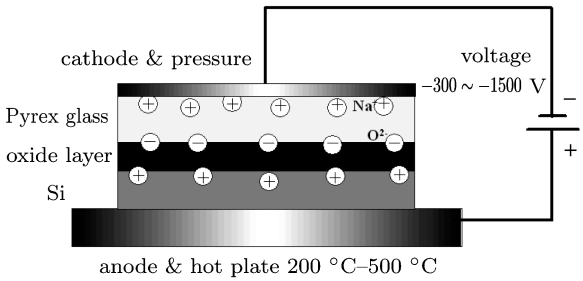


Fig. 2. Schematic illustration of anodic bonding principle.

2.2. Fabrication procedure

The fabrication procedure is schematically shown in Fig. 3. The p-type silicon plate with $< 100 >$ crystal direction was double polished and had a thickness range of 0.5 mm to 3 mm. A through hole with diameter ranging from several hundred microns to a few millimeters was elaborated in the silicon plate by laser ablation or ultrasonically drilling. A 500 microns thick Pyrex glass plate was photolithographically patterned as the same size of silicon plate. Then the two plates were anodically bonded together as shown in Fig. 3(a).

Then, we put the mixture of RbCl and BaN_6 into the hole to obtain pure Rb metal as well as N_2 buffer gas (Fig. 3(b)). The process of the reaction between these two chemicals can be summarized as following:

$$BaN_6 \xrightarrow{200^\circ C} Ba + 3N_2 \uparrow, \quad (1)$$

$$2RbCl + Ba \xrightarrow{250-300^\circ C} 2Rb \uparrow + BaCl_2. \quad (2)$$

These chemical reactions are first employed to fill the alkali vapour cells by Knappe *et al.*,[18] where they used $^{87}RbCl$ as the reactant and consequently obtained ^{87}Rb. Here we used the common chemical RbCl (99% purity, Alfa Aesar) to generate natural mixture of Rb isotopes to demonstrate the feasibility of our experimental procedure. The mixture is composed of RbCl and BaN_6 powder with the stoichiometric ratio according to the above equations (the mass ratio of RbCl to BaN_6 is 1: 0.92), and made by mixing them together through grinding, or dissolving them into water to form a clear colourless solution which was then baked to produce white solid powder.

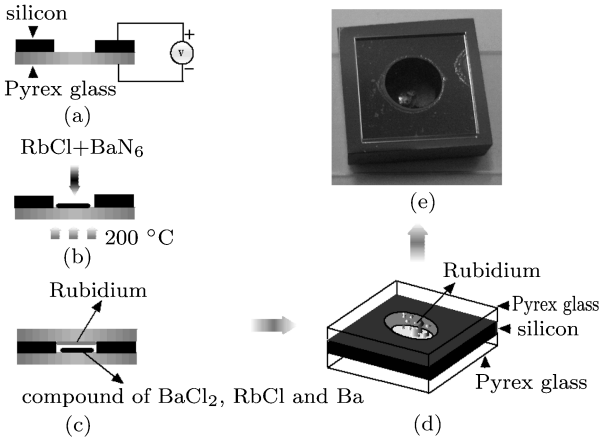


Fig. 3. Schematic illustration of the Rb vapour cell fabrication procedures. (a) Holed-silicon plate was anodically bonded to a Pyrex glass; (b) The compound of RbCl and BaN_6 was put into the hole and heated at 200 °C to release N_2; (c) The second Pyrex glass plate was bonded to complete the sealing; (d) A completed cell with metal drops in the inside surface of one Pyrex glass plate; (e) The photo of a completed cell.

After putting the compound into the hole, we placed the plate on the hot plate in the high vacuum chamber and connected it to electrodes. The pressure of the chamber can reach 4.5×10^{-4} Pa which is low enough to avoid the oxidation of Rb. The modulatory ranges of the hot plate temperature and the voltage between electrodes are large enough to ensure the anodic bonding. At first, the hot plate was heated to 200°C and kept for a few hours to make sure that BaN_6 was decomposed into N_2 and Ba completely, and the change of the pressure in the chamber was monitored by vacuum gauge to ensure there was enough N_2 being left as buffer gas in the mean time. Then, the open side of the hole is covered with the second Pyrex glass, the temperature of the hot plate was increased to 250 °C, and 1000 V voltage was applied to

initiate the anodic bonding to seal the hole hermetically. The reaction of RbCl and Ba to produce pure Rb vapour occurred at the same time. Subsequently, we left the sealed assembly in the chamber at around 300 °C for 30 minutes or more to guarantee the compound was reacted completely (Fig. 3(c)). Finally, a three-layered Rb vapour cell was obtained with metal drops coagulating on the internal surface of one Pyrex glass (Figs. 3(d) and 3(e)).

2.3. Physics package of CSAC

The microfabricated ^{85}Rb vapour cells were used to realize the physics package of CSAC. As shown in Fig. 4, the vertical cavity surface emitting laser (VCSEL) generated the light of 795 nm which was collimated and polarized by two polarizers and a quarter-wave plate before it entered the cell. The output of the light was 2 mm in diameter with circular polarization and a power of 8 μW. The photodiode behind the ^{85}Rb vapour cell was to measure the transmitted light intensity. In order to reduce the influence of exterior magnetic fields on the Zeeman energy levels of Rb atoms, we used the permalloy to make the magnetic shield around the vapour cell. Two planar heaters were fixed on the two sides of the vapour cell to control its working temperature. By integrating this physics package with the frequency stability measurement system, we can value the quality of the microfabricated vapour cells through the obtained frequency stability.

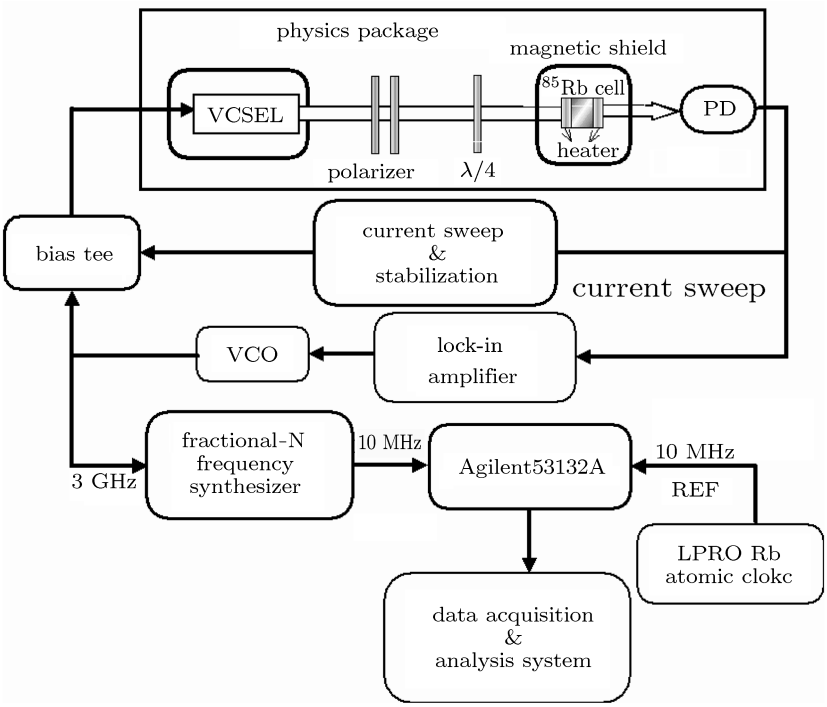


Fig. 4. Schematic illustration of the physics package of the CSACs and the frequency stability measurement system.

3. Experimental results and discussion

3.1. Observation of the Rb metal in the Cell

Figure 5 shows the photograph of a typical Rb vapour cell sealed successfully, in which the shiny drops on the inside surface of one Pyrex plate are the metallic Rb, and the black solid materials besides the Rb drops are the compound of Ba, $BaCl_2$, and minimum unreacted RbCl. In Fig. 5, we use a micromachined cell with a 3 mm-diameter hole in order to show the rubidium metal drops more clearly.

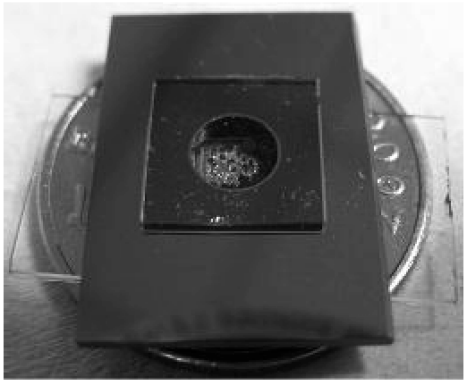


Fig. 5. Photograph of a sealed cell (10 mm×20 mm, 1 mm thick) on a 1jiao RMB coin. Shiny Rb drops are visible.

3.2. Optical absorption resonance

The existence of Rb and N_2 produced from chemical reaction in the cell was confirmed by optical absorption spectroscopy. Figure 6 shows the schematic illustration of experimental setup for measuring the optical absorption resonance and CPT resonance frequency in ^{85}Rb vapour cells. By modulating the sweeping current, the wavelength of the commercial VCSEL was scanned over the ^{85}Rb D1 transition at 795 nm. Then the laser beam passed through the vapour cell, which was heated to a controlled temperature ranging from room temperature to 120 °C, and the transmitted light power was recorded using a photodiode and shown on a oscilloscope at the same time.

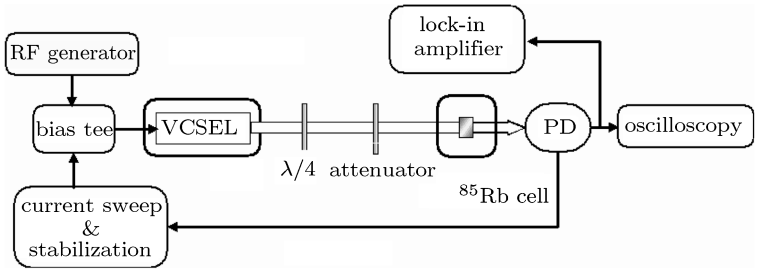


Fig. 6. Schematic illustration of experimental setup for measuring the optical absorption resonance and CPT resonance frequency.

The typical optical absorption resonances of ^{85}Rb are shown in Fig. 7.

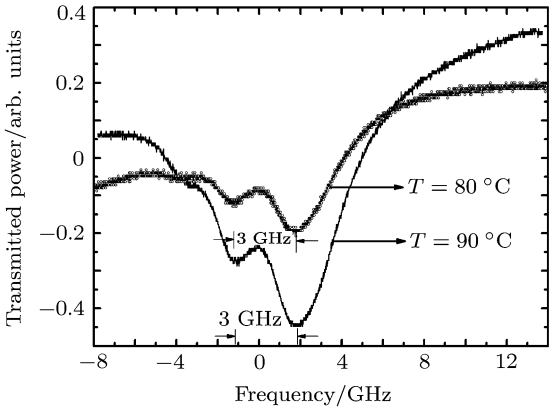


Fig. 7. Characteristic optical absorption spectra of ^{85}Rb vapour cells at different temperatures, under buffer gas pressure below 10^2 kPa.

At 80 °C, the two absorption resonance of ^{85}Rb separated by the ground state hyperfine splitting, 3.035 GHz, began to be observed. With the temperature increase, the two absorption lines enhanced gradually. The absorption became obvious at 90 °C. The full width at half maximum (FWHM) of each of the absorption resonance is about 1 GHz at 90 °C. We could evaluate the pressure of the buffer gas by comparing the broadening of the absorption line with the Rb cell made without buffer gas.[20] By using the estimation method in Ref. [20], the buffer gas pressure in this cell is estimated to be below 10^2 kPa. With such amount of buffer gases in vapour cells, we can lock the laser wavelength on the right transition so that it is possible to detect CPT signals.

3.3. CPT Resonance

Figure 8 shows the CPT resonance detected in a successfully-fabricated cell. In this experiment, the VCSEL beam (2 mm in diameter) is circularly polarized and attenuated, leaving only 50 μW before entering the vapour cell. With the modulation of sweeping current, a substantial fraction of the laser power is transferred to the sidebands from the carrier band.

By locking the VCSEL beam frequency on the absorption spectrum, the first sideband is roughly matched with the transition to create the resonance. The cell we used for the detection of CPT resonance (Fig. 8) is 1 mm thick and 3 mm in diameter, the internal volume is 6.97 mm^3. We also obtained CPT signals from cells with different thicknesses of 500 μm and 3 mm respectively. In Fig. 8(a), the observed FWHM of the CPT resonance is about 1.7 kHz, and the calculated contrast is about 1.5% at 90 °C. Figure 8(b) shows its related error signal. The later CSAC physics package tests have proved that the cells with such narrow linewidth are of good quality in the use of CSACs.

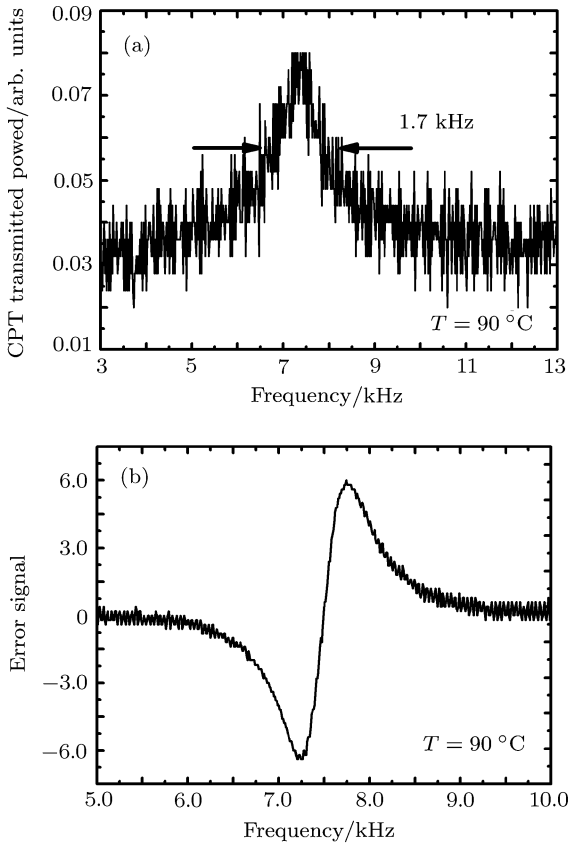


Fig. 8. (a) Measured CPT resonance signal of the cell (3 mm in diameter, 1 mm in length) has width of 1.7 kHz and signal contrast of 1.5% at 90 °C; (b) Related error signal.

3.4. Sealing quality of the cells

The sealing quality of miniaturized Rb cells fabricated based on anodic bonding technique is very important in their realization of CSACs and long-term stable use. We valuated the sealing quality by a helium leaking detection method.

Helium-filled cells were fabricated in the chamber with a helium pressure of 2×10^4 Pa. Then, their helium leaking rates were measured by using Helium Leak Detector ASM-192TD$^+$ (Alcatel Vacuum Technology, France) at 26 °C. The minimum detectable helium leakage of the detector is 2.0×10^{-11} Pa·m^3/s. At first, we got a based helium signal without the cell in the detector's chamber. Then, we obtained another helium signal after putting the cell into the detector chamber. These two values were the same, by which we estimated that the cell's helium leak rate is at least lower than 2.0×10^{-11} Pa·m^3/s. The lifetime of the cell can be valuated by the following function:

$$T = \frac{Vp}{q},$$

where T is the lifetime of the cell, V is the volume of the cell, p is the helium pressure in the cell, and q is the detectable helium leak of the cell. The internal volume of the cell is about 6.97 mm^3 as mentioned in subsection 3.3. Both p and q are given by our helium leaking detection experiment described above so that the calculated T is more than 81 days, which can satisfy our experimental requirement.

The actual lifetime is much longer than this estimated result, which is demonstrated by our subsequent experimental detection. Figure 9 shows the CPT resonance signal of the same cell whose CPT signal is shown in Fig. 8(a), but it was measured nine months later. We can see that the linewidth is nearly the same as the original one, which suggests that the sealing quality and stability of the cells are qualified enough for the CSACs use in the next step.

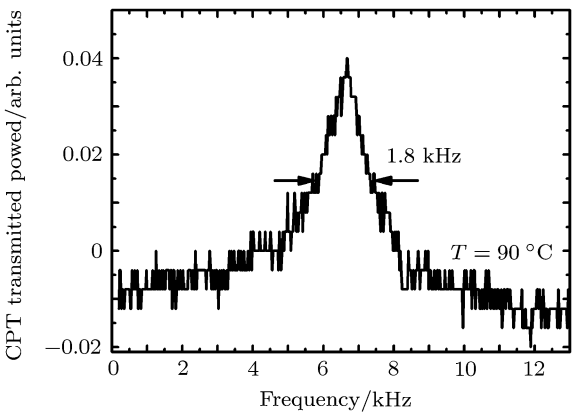


Fig. 9. The CPT resonance signal of the same cell mentioned in Fig. 7 measured 9 months later.

3.5. Frequency stability of the CSACs

We established the frequency stability measurement system for the CSAC, as shown in Fig. 4, to prove the quality of the microfabricated vapour cells.

This system takes the LPRO Rb atomic clock as the frequency reference and is controlled by the Labview environment on PC to perform the measurement and record the results automatically. Matlab is employed to process the experiment result to calculate the frequency stability.

In Fig. 4, the output of the PD is divided into two feedback loops. One loop is to lock the wavelength of the laser on the absorption resonance through the lock-in amplifier and current source to stabilize the control current of the laser. The other loop is to lock the VCO frequency to the ^{85}Rb hyperfine splitting frequency. The ground state hyperfine splitting frequency of 3.035 GHz is divided into a standard frequency of 10MHz through Fractional-N frequency synthesizer. Then, the signal is transmitted to the Time Interval/Frequency Counter Agilent53132A with a LPRO Rb atomic clock as the reference to record the experimental results. Finally, the results are analysed by Matlab program and the frequency stability could be obtained.

The data points marked by small squares in Fig. 10 shows the Allan deviation of the CSAS physics package based the microfabricated Rb vapour cell, which was 1 mm thick and 3 mm in diameter, at a heating temperature of 100 °C. The Allan deviation can reach to 2.1×10^{-10} at 1 s, and the deviation is in the scale of 1×10^{-11} to 1×10^{-10} at longer times ($\tau > 50$ s). These results are comparable to that of a glass-blowing Rb vapour cell, whose diameter of section is 1 cm and length is 1 cm, at 40 °C (the data points marked with dots in Fig. 10). Therefore, the Rb vapour cells fabricated by anodic bonding are of good quality for the use of CSACs. Although the power consumption of the microfabricated cell is larger than that of the glass-blowing cell, this kind of the cell can reduce the volume of the physics package of CSAC greatly. In the later experiment, we can reduce the total power consumption by improving the temperature control part of this system.

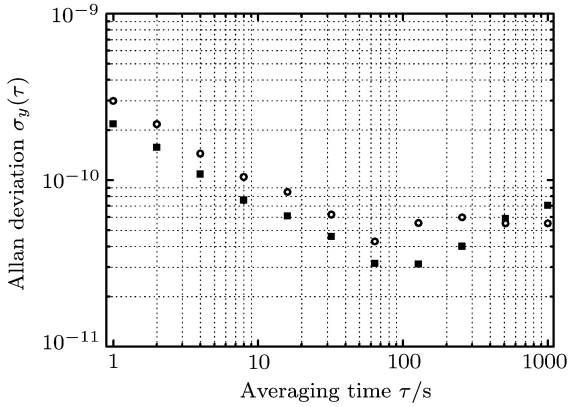


Fig. 10. Measured Allan deviation of the CSAC physics package based on the microfabricated Rb vapour cell at 100 °C (squares), and the glass-blowing vapour cell at 40 °C (dots).

4. Conclusions

We fabricated sandwich-structured ^{85}Rb vapour cells successfully by using the anodic bonding technique and *in situ* chemical reaction between RbCl and BaN_6 to produce pure Rb metal and buffer gases. The optical absorption resonance of ^{85}Rb was detected in the sealed cells. Moreover, we obtained the CPT resonance signal with contrast of 1.5% and FWHM of about 1.7 kHz at 90 °C, which suggests that this kind of cells can be used in CPT atomic clocks. The low leak rate (less than 2.0×10^{-11} Pa·m^3/s) and long lifetime (more than 9 months) of the cells make sure of their long-term and stable use in CSACs. In addition, we realized the physics package of CSAC by integrating the cell. At a heating temperature of 100 °C, the measured Allan deviation can reach to 2.1×10^{-10} at 1 s, and the deviation is in the scale of 1×10^{-11} to 1×10^{-10} at longer times($\tau > 50$ s). Thus, the cell was proved to have the quality to be used in portable and battery-operated devices. Since the kinds and partial pressures of buffer gases can significantly influence the long-term stability of the atomic clocks, we will try to control the buffer gases more precisely in the cells in the next step, and also broaden their application range to other kinds of frequency instruments based on atomic excitation.

References

[1] Fruehauf H 2001 *Proc. 33rd Annual Precise Time Interval (PTTI) Systems and Applications Meeting* (Ling Beach, CA) p359

[2] Kusters J A and Adams C A 1999 *RF design* p28

[3] Kitching J, Knappe S and Hollberg L 2002 *Appl. Phys. Lett.* **81** 553

[4] Cyr N, Tetu M and Breton M 1993 *IEEE Trans. Inst Meas.* **42** 640

[5] Zhu M and Cutler L S 2000 *Proc. 32nd Annual Precise Time and Time Interval (PTTI) Systems and Applications Meeting* (Reston, Virginia, USA) p311
[6] Goka S, Okura T, Moroyama M and Watanabe Y 2008 *IEEE International Frequency Control Symposium* (Honolulu, Hawaii, USA) p103
[7] Seigneur F, Carazzetti P, Schori C, Maeder T, Mileti G, Thomann P and Shea H R 2009 *Transducers* Paper ID 1836
[8] Lutwak R, Emmons D, English T, Riley W, Duwel A, Varghese M, Serkland D K and Peake G M 2003 *Proc. of the 35th Annual Precise Time and Time Interval (PTTI) Systems and Applications Meeting* (San Diego, California) p467
[9] Knappe S, Velichansky V, Robinson H G, Liew L, Moreland J, Kitching J and Hollberg L 2003 *Proc. of the 2003 IEEE International Frequency Control Symposium and PDA Exhibition Jointly with the 17th European Frequency and Time Forum* (Tempa, Florida, USA) p31
[10] Liew L A, Knappe S, Moreland J, Robinson H, Hollberg L and Kitching J 2004 *Appl. Phys. Lett.* **84** 2694
[11] Liew L A, Moreland J and Gerginov V 2007 *Appl. Phys. Lett.* **90** 114106
[12] Douahi A, Nieradko L, Beugnot J C, Dziuban J, Maillote H, Guerandel S, Moraja M, Gorecki C and Giordano V 2007 *Electron. Lett.* **43** 279
[13] Gong F, Jau Y Y, Jensen K and Happer W 2006 *Rev. Sci. Instrum.* **77** 076101
[14] Lutwak R, Emmons D, Riley W and Garvey R M 2002 *Proc. of the 34th Annual Precise Time and Time Interval (PTTI) Systems and Applications Meeting* (Reston, Virginia) p539
[15] Stahler M, Wynands R, Knappe S, Kitching J, Hollberg L, Taichenachev A and Yudin V 2002 *Opt. Lett.* **27** 1472
[16] Lee C H, Guo H, Radhakrishnan S, Lal A, Szekely C, McClelland T and Pisano A P 2004 *Proc. to the Solid State Sensor, Actuator and Microsystems Workshop* (Hilton Head Island, SC) p23
[17] Padhakrishnan S and Lal A 2005 *Proc. of the 13th International Conference on Solid-State Sensors, Actuators and Microsystems* (Seoul, Korea) p23
[18] Knappe S, Schwindt P D D, Shah V, Hollberg L, Kitching J, Liew L and Moreland J 2005 *Opt. Express* **13** 1249
[19] Wang X H, Chen X Z, Hou J D, Yang D H and Wang Y Q 2000 *Acta Phys. Sin.* **49** 0085 (in Chinese)
[20] Deng K, Guo T, He D W, Liu X Y, Liu L, Guo D Z, Chen X Z and Wang Z 2008 *Appl. Phys. Lett.* **92** 211104
[21] Deng K, Guo T, Su J, Guo D Z, Liu X Y, Liu L, Chen X Z and Wang Z 2009 *Phys. Lett.* A **373** 1130
[22] Yi L, Yuan J, Qi X H, Chen W L, Zhou D W, Zhou T, Zhou X J and Chen X Z 2009 *Chin. Phys.* B **18** 1409
[23] Camparo J C and Coffer J G 1999 *Phys. Rev.* A **59** 728
[24] Wallis G and Pomerantz D I 1969 *J. Appl. Phys.* **40** 3946
[25] Schmidt M A 1998 *Proc. IEEE* **86** 1573
[26] Kanda Y, Matsuda K, Murayama C and Sugaya J 1990 *Sens. Actuat.* **23** 939